ELSEVIER

Thin Solid Films 258 (1995) 56–63

thin solid films

Structures of tantalum pentoxide thin films formed by reactive sputtering of Ta metal

Peng-Heng Chang[a], Hung-Yu Liu[b]

[a]Institute of Materials Science and Engineering, National Chiao Tung University, Sinchu, Taiwan
[b]Materials Science Laboratory, PO Box 655936, Mail Station 147, Texas Instruments Inc., Dallas, TX 75265, USA

Received 31 March 1994; accepted 11 October 1994

Abstract

Reactively sputtered Ta_2O_5 films adhere poorly on bare Si substrate, but the adhesion improves dramatically on a thermally oxidized Si surface. The films are non-stoichiometric and the atomic ratio of O to Ta is typically higher than 2.5 but decreases with increasing annealing temperature. The variation in non-stoichiometry is also reflected by a small decrease in lattice constants with increasing annealing temperature as revealed by X-ray diffraction. About 2 at.% of residual Ar is detected in Ta_2O_5 film formed by 70%Ar–30%O_2 sputtering. The as-deposited Ta_2O_5 film is amorphous and it transforms to crystalline Ta_2O_5 at temperatures higher than 600 °C. Crystalline Ta_2O_5 films contain numerous amorphous particles which have been previously incorrectly identified as voids. They are probably the remnants of the uncrystallized amorphous Ta_2O_5 materials. The amorphous particles have a bimodal size distribution and the average size increases with increasing annealing temperature. The deterioration of dielectric properties in crystallized Ta_2O_5 films is unlikely to arise from these amorphous particles because amorphous Ta_2O_5 is known to have very low leakage current. An interfacial SiO_2 layer forms at the Ta_2O_5–Si interface during reactive sputtering and its thickness increases with increasing oxygen content in the sputtering gas. Annealing at high temperature in Ar ambient has little effect on the thickness of this interfacial SiO_2 layer.

Keywords: Dielectrics; Oxides; Structural properties; Tantalum

1. Introduction

Tantalum oxide films are of interest for applications in high temperature resistance [1], anti-reflection coatings for solar cells [2], optical waveguides [3], oxygen sensors [4], and capacitor dielectric materials [5]. In recent years they have received increasing attention as an alternative dielectric to replace thin SiO_2 films for storage capacitors in very large-scale-integrated memory cells and as gate insulators in metal–oxide–semiconductor devices [6, 7]. Tantalum oxide films can be formed by at least five different methods: (1) thermal oxidation of sputtered tantalum films [4, 8–10]; (2) chemical vapor deposition (CVD) using a $TaCl_5$ [11], $Ta(OC_2H_5)_5$ [12] or $TaCl_2(OC_2H_5)_2C_5H_7O_2$ [13] source; (3) anodization of Ta metal films [14–16]; (4) magnetron sputter deposition from a Ta_2O_5 target using reactive O_2–Ar gas [17]; and (5) reactive sputtering of a pure Ta target using O_2–Ar gas [18,19].

Ta_2O_5 film formed by thermal oxidation of Ta metal is usually amorphous if oxidized below 600 °C, but it crystallizes with deteriorating electrical properties (higher leakeage current and lower breakdown voltage) when annealed in inert or oxidizing ambients [20, 21]. The crystallization process is apparently thermally activated for it requires 14 h at 600 °C but less than 30 min at 900 °C [20]. Thermal oxidation of Ta metal deposited on an Si substrate not only produces aTa_2O_5 film but also an interfacial SiO_2 layer is formed at the Ta_2O_5–Si interface [21]. A similar interfacial SiO_2 layer is also observed when Ta_2O_5 is formed by reactive sputtering of a Ta target [22]. In the latter case, the Ta_2O_5 film is always amorphous in the as-deposited condition but crystallizes upon annealing at tempera-

0040-6090/95/$9.50 © 1995 — Elsevier Science S.A. All rights reserved
SSDI 0040-6090(94)06402-4

tures in excess of 600 °C [23]. Like thermal oxide, the reactively sputtered tantalum oxide also exhibits inferior electrical properties in crystalline form [24].

Anodic tantalum oxide is also amorphous in general, but prolonged anodization at constant voltage will cause crystalline Ta_2O_5 to grow at the oxide–Ta interface [25–27]. The crystalline anodic Ta_2O_5 is not produced by the crystallization of existing amorphous Ta_2O_5 but is a new oxide growing at the interface between the Ta substrate and the amorphous Ta_2O_5 layer and it physically displaces and spalls the overlaying amorphous oxide [27]. The amorphous anodic tantulum oxide can be crystallized by thermal treatment at temperatures higher than 500 °C [28]. CVD Ta_2O_5 has the advantage of better step coverage compared with other types of Ta_2O_5 film, but it shows poor d.c. conduction behavior (i.e. much higher leakage current) [12, 13, 29]. CVD Ta_2O_5 films formed at low temperatures (<500 °C) tend to be amorphous [13, 30] while those formed at higher temperatures are crystalline [30, 31]. Recently it was found that the leakage current of CVD Ta_2O_5 can be greatly reduced by a two-step anneal using ozone and dry O_2 [12].

In this paper the structure of Ta_2O_5 films formed by reactive sputtering of a Ta target is studied. Several advanced characterization techniques, such as thin film X-ray diffraction, Rutherford backscattering spectrometry (RBS) and high resolution transmission electron microscopy (HRTEM), are employed synergistically to provide a comprehensive picture of the structural evolution of the oxide films during rapid thermal annealing.

2. Experimental procedure

Tantalum pentoxide films were formed by d.c. magentron sputtering of a pure Ta target using reactive O_2–Ar gas. The substrates were 100 mm in diameter, p-type, Si{111} wafers with or without a thermally grown SiO_2 layer. Table 1 summarizes the substrates and sputtering gas compositions for the four groups of wafers studied. To facilitate the following discussions they are designated as A, B, C and D series. The nominal thickness of Ta_2O_5 film was 100 nm, constant across the series. The nominal thickness of the thermally grown SiO_2 layer was 35 nm in the C and D series. The films were subsequently rapidly thermally annealed for 10 s in an Ar ambient at 600, 800 or 1000 °C, using separate wafers for each temperature. The structures of the as-deposited and the annealed wafers were examined by thin film X-ray diffraction, transmission electron microscopy (TEM), and RBS. The detailed procedures of these analyses were similar to those reported previously [32].

Table 1
Substrates and sputtering gas composition

Series	Substrate	Gas composition
A	Si	70%Ar–30%O_2
B	Si	100%O_2
C	SiO_2/Si	70%Ar–30%O_2
D	SiO_2/Si	100%O_2

3. Results and discussion

The X-ray diffraction patterns obtained from the four series are similar for the same annealing conditions, irrespective of the differences in substrate and sputtering gas composition. For the sake of brevity, we will only demonstrate the results for the D series at three different annealing temperatures, as shown in Fig. 1. The pattern for the as-quenched sample is not shown because it is practically the same as for the sample annealed at 600 °C. It is clear from Fig. 1 that Ta_2O_5 film is amorphous below 600 °C as implied by the broad diffuse-scattering background of the 600 °C spectrum. Annealing at 800 or 1000 °C results in the crystallization of the films as revealed by the appearance of diffraction peaks in the 800 and 1000 °C spectra. All the peaks shown in Fig. 1 can be ascribed to the orthorhombic Ta_2O_5 phase with lattice constants $a = 0.6198$ nm, $b = 4.029$ nm and $c = 0.3888$ nm [33]. The reflecting lattice plane(s) corresponding to the peaks are also labeled in Fig. 1. Close examination of the 800 and 1000 °C spectra in Fig. 1 reveals a small shift of peak positions toward lower 2θ angle. This implies a decrease of lattice constants for the crystalline Ta_2O_5 films as the annealing temperature is increased. This variation of lattice constants is probably due to the change in non-stoichiometry of the films upon annealing.

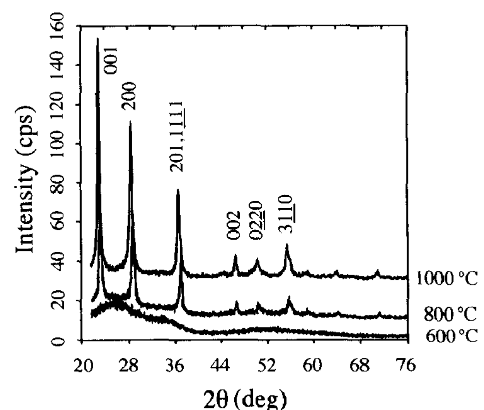

Fig. 1. Thin film X-ray diffraction patterns of Ta_2O_5 films annealed at three different temperatures. The films were sputtered on Si substrates using pure oxygen gas.

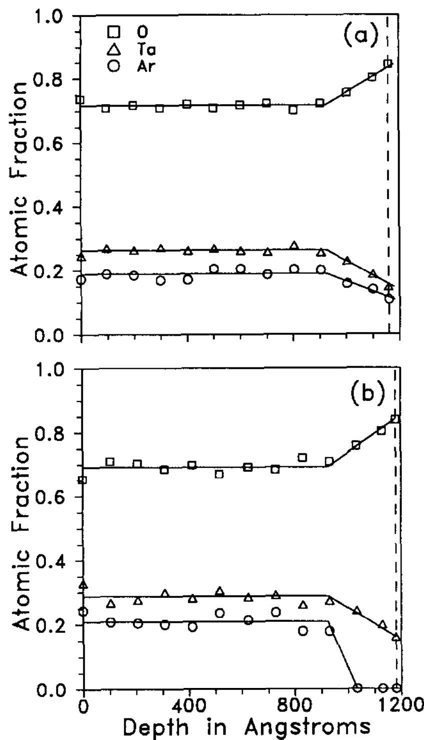

Fig. 2. RBS depth profile of a Ta_2O_5 film formed by $Ar-O_2$ sputtering on an SiO_2 substrate and annealed at (a) 600 °C and (b) 1000 °C. The atomic fraction scale for Ar is expanded by a factor of 10.

The stoichiometry of the films can be determined by RBS depth profiling. Because of the poor film quality in the A and B series, RBS depth profiling was performed only on the C and D series. Fig. 2 and Fig. 3 show the concentration profiles of samples annealed at 600 and 1000 °C for the C and D series respectively. The vertical broken line in each figure represents the $Ta_2O_5-SiO_2$ interface as determined by TEM. It is evident that films formed by $Ar-O_2$ sputtering (Fig. 2) contain about 2 at.%Ar, which is not present in films sputtered by pure O_2 (Fig. 3). The Ar concentration in Fig. 2 remains at about 2 at.% independent of annealing temperature, which is not unexpected in view of the short annealing time (only 10 s). The concentration of Ta and oxygen is fairly constant throughout the Ta_2O_5 film in each case, except near the $Ta_2O_5-SiO_2$ interface. Using the concentrations in the bulk of the film for calculation, the O/Ta ratio is found to be 2.71 and 2.85 at 600 °C for the C and D series respectively. This ratio is decreased to 2.65 and 2.68 at 1000 °C for the C and D series respectively. The change in the lattice constants of the films as revealed by the X-ray results discussed previously is very likely related to this variation in non-stoichiometry.

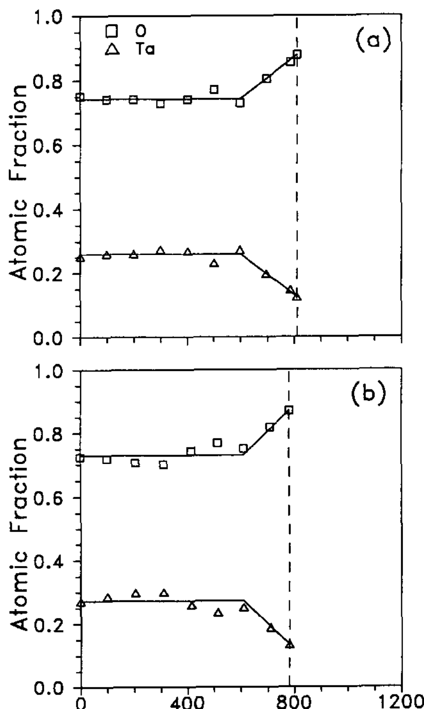

Fig. 3. RBS depth profile of a Ta_2O_5 film formed by pure O_2 sputtering on an SiO_2 substrate and annealed at (a) 600 °C and (b) 1000 °C.

The cross-sectional TEM microstructures of the Ta_2O_5 films formed on bare Si substrates (A and B series) and annealed at different temperatures are shown in Fig. 4 and Fig. 5 respectively. Several observations can be made from these figures, as follows.

(1) Although the original substrate is a bare Si wafer, a thin layer of SiO_2 is formed at the Ta_2O_5-Si interface as a result of the reactive sputtering. The thickness of the SiO_2 layer changes little with increasing annealing temperature, indicating that it is formed during the sputtering. This result is in agreement with that of others [9] who had shown that oxygen would diffuse through Ta_2O_5 film during reactive sputtering to oxidize the underlying Si substrate. The SiO_2 thickness increases with increasing O_2 content in the sputtering gas, being 8 nm for the $Ar-30\%O_2$ gas and 18 nm for the pure O_2 case.

(2) The adhesion of the films to Si is poor. Delamination is observed even in the as-deposited condition. Annealing the films at higher temperature worsens adhesion. Films formed by pure O_2 sputtering are worse than those formed by $Ar-O_2$ sputtering. Note that delamination is not at the $Ta_2O_5-SiO_2$ interface, but is inside the Ta_2O_5 film about 10 nm away from the interface.

(3) Consistent with the X-ray results, the as-deposited films and films annealed at 600 °C are amorphous. Films annealed at 800 and 1000 °C showed evidence of crystallinity.

(4) Pore-like features are formed in the crystalline Ta_2O_5 film. They are discernible in the samples annealed at 800 °C and become evident in the sample annealed at 1000 °C.

The films formed on oxidized Si wafers and annealed at different temperatures are shown in Fig. 6 and Fig. 7

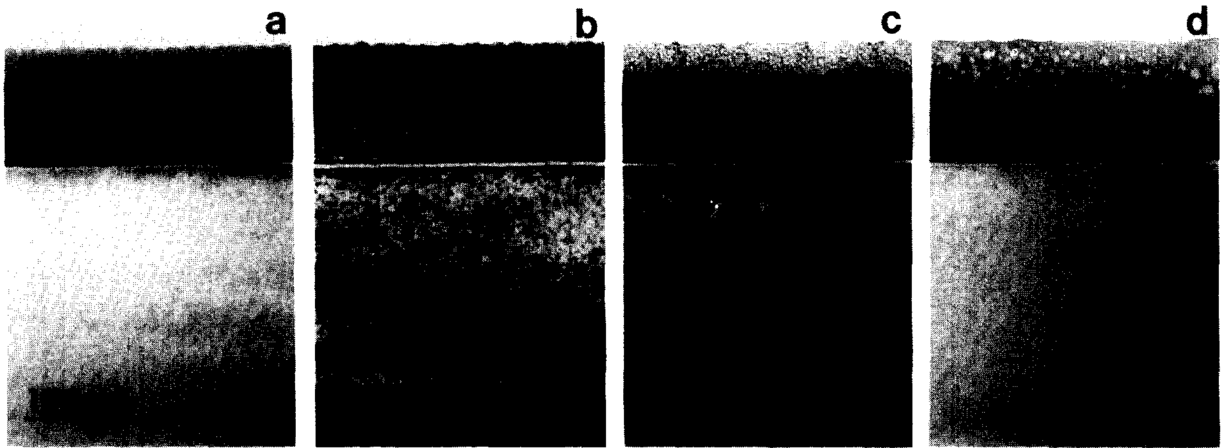

Fig. 4. Cross-sectional TEM microstructure of Ta_2O_5 films formed on Si substrates by Ar–O_2 sputtering: (a) as-deposited film; (b)–(d) films rapidly thermally annealed for 10 s at (b) 600 °C, (c) 800 °C and (d) 1000 °C.

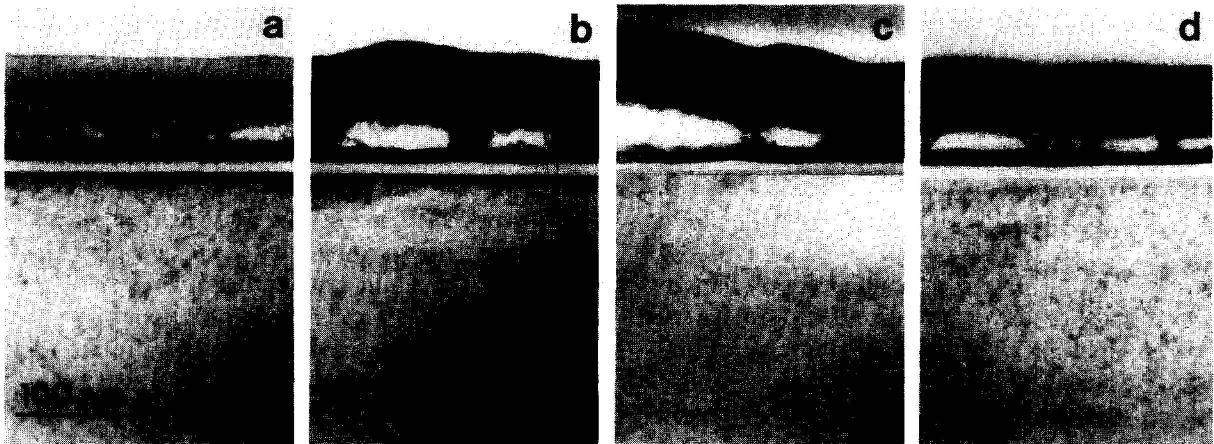

Fig. 5. Cross-sectional TEM microstructure of Ta_2O_5 films formed on Si substrates by pure O_2 sputtering: (a) as-deposited film; (b)–(d) films rapidly thermally annealed for 10 s at (b) 600 °C, (c) 800 °C and (d) 1000 °C.

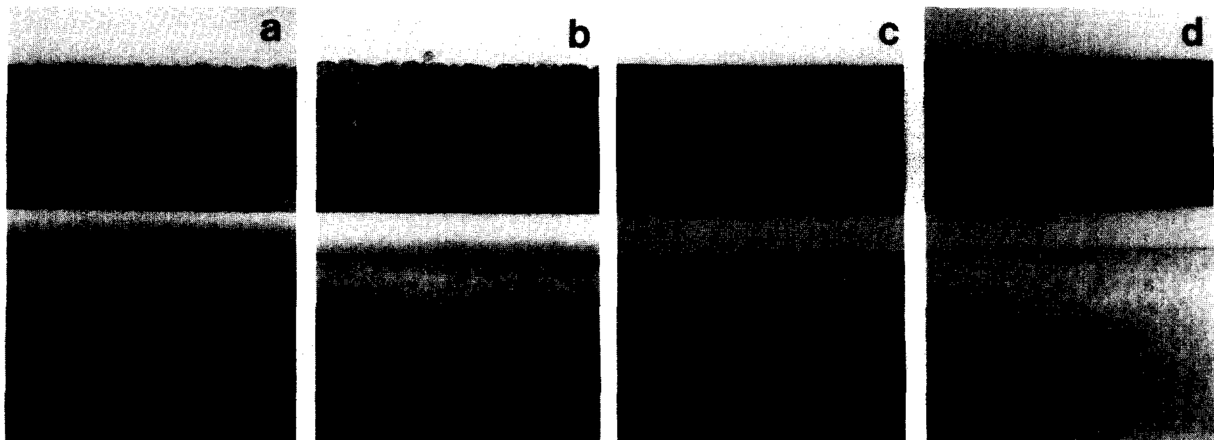

Fig. 6. Cross-sectional TEM microstructure of Ta_2O_5 films formed on SiO_2 substrates by Ar–O_2 sputtering: (a) as-deposited film; (b)–(d) films rapdily thermally annealed for 10 s at (b) 600 °C, (c) 800 °C and (d) 1000 °C.

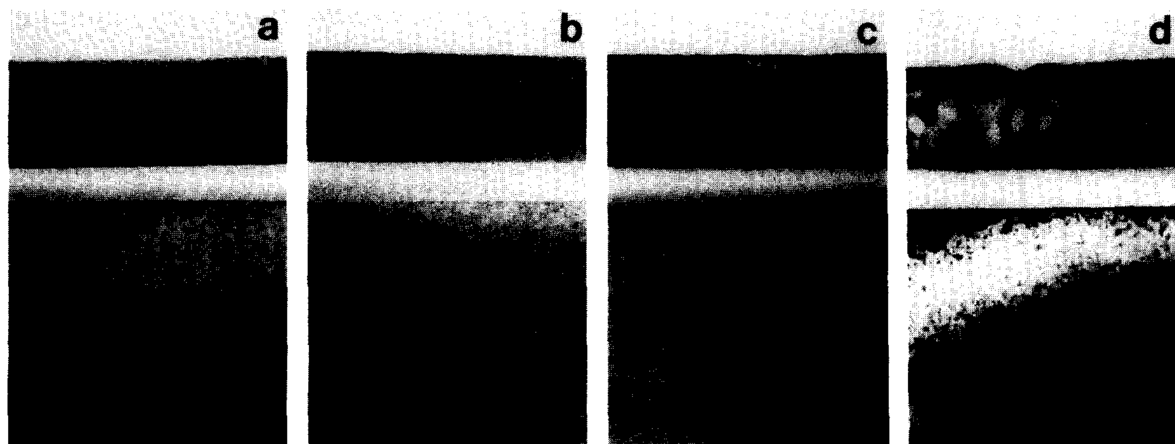

Fig. 7. Cross-sectional TEM microstructure of Ta_2O_5 films formed on SiO_2 substrates by pure O_2 sputtering: (a) as-deposited film; (b)–(d) films rapidly thermally annealed for 10 s at (b) 600 °C, (c) 800 °C and (d) 1000 °C.

for Ar–O_2 (C series) and pure O_2 (D series) sputtering respectively. Comparing these two figures with Figs. 4 and 5, it is apparent that the presence of thermal oxide on the substrate improves the adhesion of the Ta_2O_5 films dramatically. Delamination is not observed in any of the micrographs shown in Figs. 6 and 7 and the film quality is excellent. Pore-like features are also present and they seem to appear at lower temperature in the pure O_2 sputtered films than in the (Ar–O_2)-sputtered films.

Close examination of the crystalline Ta_2O_5 films by HRTEM reveals that the pore-like features are not voids. Fig. 8 shows a typical high resolution transmission electron micrograph of the structure within a Ta_2O_5 grain and the pore-like features are unequivocally amorphous in nature. In the conventional transmission electron micrographs shown in Figs. 4–7 many of these features appear to be faceted, but in HRTEM the faceting is less obvious. Numerous amorphous particles are also located at grain boundaries, and a typical example is shown in Fig. 9 (the edges of the amorphous particles sometimes exhibit lattice fringes due to the overlapping of crystalline materials over amorphous regions). The grain boundary particles extend into grains on both sides of the boundary and are much larger in size than those located in the grain interior. The bimodal size distribution of the amorphous particles is best revealed in Fig. 10 which shows plane view transmission electron micrographs of a film annealed at 1000 °C. The grain boundaries in Fig. 10(a) are decorated with many large irregular-shaped amorphous particles while smaller particles in the grain interior can be easily identified in Fig. 10(b).

Pore-like features have been previously observed by others in Ta_2O_5 films formed by r.f. magnetron sputtering of a pure Ta target using Ar–O_2 gas [23, 24]. We

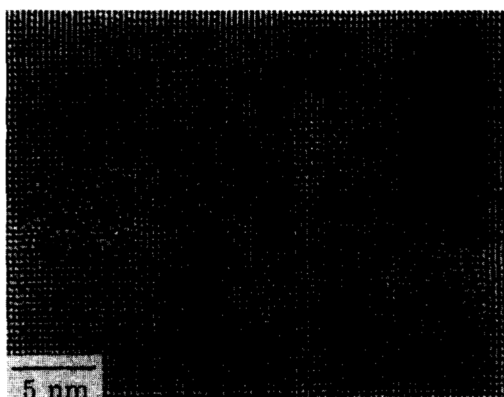

Fig. 8. Planar high resolution transmission electron micrograph showing the structure of crystalline Ta_2O_5 film within a grain. The film was formed by Ar–O_2 sputtering on an SiO_2 substrate and subsequently annealed at 1000 °C.

Fig. 9. Planar high resolution transmission electron micrograph showing the structure of crystalline Ta_2O_5 film at grain boundaries. (The grain boundaries are marked by pairs of triangles). The film was formed by Ar–O_2 sputtering on an SiO_2 substrate and subsequently annealed at 1000 °C.

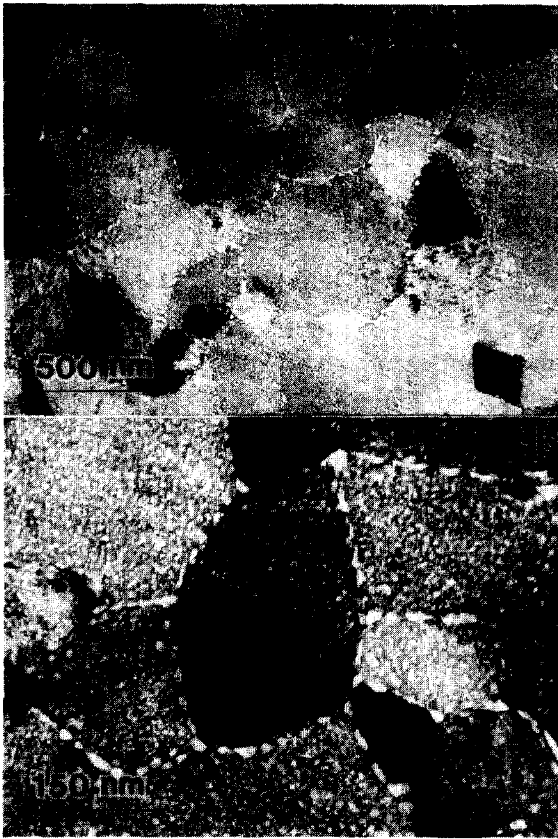

Fig. 10. Planar TEM microstructure of Ta_2O_5 films formed on Si substrates by Ar–O_2 sputtering and annealed at 1000 °C; (b) is a blow-up of (a).

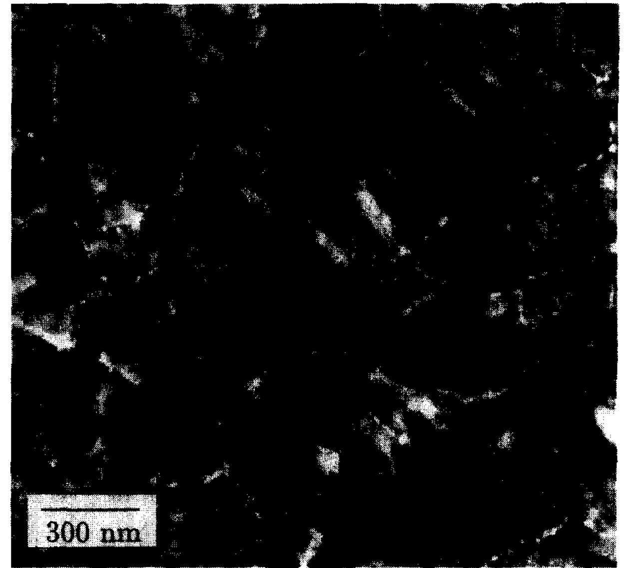

Fig. 11. Planar TEM microstructure of Ta_2O_5 film formed on an Si substrate by thermal oxidation of Ta metal film at 1000 °C for 1 h in a dry oxygen ambient.

have also observed similar features in Ta_2O_5 films formed by high temperature thermal oxidation of Ta films [34]. Fig. 11 shows a Ta_2O_5 film formed by thermally oxidizing an electron-gun-evaporated Ta film at 1000 °C for 1 h in dry oxygen ambient. The substrate of this sample is a 3 in Si < 100 > wafer and the Ta thickness is 30 nm. The oxidation in this case is long enough to convert Ta completely to Ta_2O_5. The resemblance of the pore-like features in Fig. 11 to those in Fig. 10 is striking and their amorphous nature is also confirmed by HRTEM examinations. Additionally, we have found, consistently with others [20, 21], that the Ta_2O_5 film grown by thermal oxidation of Ta film is entirely amorphous if oxidized below 600 °C, but crystalline Ta_2O_5 film is formed at high oxidation temperatures. Like reactively sputtered Ta_2O_5 films, the amorphous particles are present in all crystalline Ta_2O_5 films formed by thermal oxidation in our observations. In the past, the pore-like features were identified as voids by their appearance in TEM. (The amorphous nature makes the particles featureless and they appear much whiter than the surrounding crystalline Ta_2O_5 when viewed in TEM, so it is very easy to have mistaken them as voids.) Under this incorrect presumption several hypotheses have been advanced to explain their origin. These include: (1) they are preciptates of Ar gas trapped in the films from the sputtering gas [23], (2) they are voids formed due to inhomeogeneity in stress distribution during the densification of the sputtered films upon annealing [24], or (3) they are voids formed by vacancy condensation [24].

Our HRTEM results, however, cast serious doubt on these hypotheses. Further supporting evidence of these features being amorphous rather than pores is the fact that Ta_2O_5 films annealed at 1000 °C contain large amounts of them (for instance, the apparent volume fraction of amorphous particles in Fig. 7(d) is over 50%) yet the film integrity is not impaired at all which is very unlikely if they were voids.

The RBS results presented earlier show clearly that the reactively sputtered Ta_2O_5 films contain only Ta and O (and Ar if Ar gas is used in the sputtering). Since Si is not detected in the Ta_2O_5 films, the possibility of the amorphous particles being SiO_2 formed by the interaction of the in-diffusing oxygen atoms and the out-diffusig Si atoms is ruled out. The facts that amorphous particles are observed in Ta_2O_5 films formed by pure O_2 sputtering and by thermal oxidation of Ta metal films in dry oxygen indicate that their origin is not related to the trapped Ar gas for Ar is not present in these films at all. However, Ar may affect the formation of the amorphous particles in an indirect way because films containing Ar seem to have fewer amorphous particles relative to films not containing Ar (comparing Fig. 4(d) with Fig. 5(d) and Fig. 6(d) with Fig. 7(d)). The fact that no elements other than Ta, O and Ar are detected by RBS strongly suggests that the

amorphous particles are the remnants of the original amorphous film not being crystallized during the high temperature heat treatment. Evidence supporting this hypothesis is presented in Fig. 12(a) which shows a planar TEM microstructure observed in a partially transformed sample annealed at 800 °C in the C series (its corresponding cross-sectional TEM microstructure has been shown in Fig. 6(c)). The area marked A in this figure is a large untransformed amorphous region surrounded by crystalline Ta_2O_5 grains. Fig. 12(b) is a close-up of the interface area between region A (upper right) and a crystalline Ta_2O_5 grain (lower left). Numerous tiny amorphous particles can be seen in the crystalline region in Fig. 12(b). From Figs. 4–7 it is evident that the size of the amorphous particles tends to increase with increasing annealing temperature (a similar trend is also observed in thermally oxidized Ta_2O_5 films [34]). This tendency is unlikely to be caused by the thermally activated dissolution and growth (Ostwald ripening) process frequently observed in solid state precipitation [35], for there is no driving force for an amorphous Ta_2O_5 particle to be dissolved into a crystaline Ta_2O_5 and subsequently to precipitate out onto other amorphous particles. The size difference of the particles at different temperatures may be due to the variation in the rate of crystallization. The faster crystallization associated with the higher temperatures seems to leave larger untransformed regions behind. The residual amorphous particles in otherwise crystalized films are very stable; we have previously shown that a 30 min oxidation treatment at 1050 °C does not crystallize them [22].

Fig. 12. Planar TEM microstructure of partially crystallized Ta_2O_5 film. The letter A denotes an amorphous region surrounded by crystallized oxide. The film was deposited on an Si substrate by $Ar-O_2$ sputtering and annealed at 800 °C.

It is well known that Ta_2O_5 films formed by reactive sputtering of a Ta target possess excellent electrical properties if they are amorphous. The electrical properties deteriorate dramatically after a high temperature anneal when the films are crystallized [22]. The amorphous particles have been blamed for the poor dielectric properties of the crystalline Ta_2O_5 films based on the incorrect identification of their being voids. Our HRTEM results cast serious doubt on this conjecture and further studies are required to clarify the cause of the large leakage current observed in the crystalline films containing amorphous particles.

4. Conclusions

(1) Reactively sputtered Ta_2O_5 films adhere very poorly on an Si substrate. The adhesion improves dramatically on a thermally oxidized Si surface. Films formed by pure O_2 sputtering have poorer quality than films formed by $Ar-O_2$ sputtering.

(2) Oxygen in the sputtering gas is found to diffuse through Ta_2O_5 and react with the substrate Si to form an SiO_2 layer at the film–substrate interface. The thickness of the interface SiO_2 layer increases with increasing oxygen content in the sputtering gas. The interfacial SiO_2 layer is formed during sputtering. Subsequent annealing at high temperatures in an Ar ambient has no effect on its thickness.

(3) Ta_2O_5 films formed by $Ar-O_2$ sputtering contains about 2 at.% Ar which remains in the film even after 1000 °C annealing.

(4) Reactively sputtered Ta_2O_5 films are non-stoichiometric. The O/Ta ratio is generally greater than 2.5 but decreases with increasing annealing temperature. This variation in stoichiometry is also reflected by a small decrease in lattice constants with increasing annealing temperature.

(5) The as-deposited Ta_2O_5 film is amorphous and remains so if annealed at temperatures below 600 °C. Higher temperature annealing transforms the film to crystalline phase with a concomitant deterioration of electrical properties.

(6) Crystalline Ta_2O_5 films contain numerous amporphous particles which have been previously incorrectly identified as voids. The particles have a bimodal size distribution and their average size increases with

increasing annealing temperature. They are very likely the remnants of the uncrystallized amorphous Ta_2O_5 materials.

Acknowledgements

This work is partially supported by the National Science Council, Taiwan, through Grant NSC 80-0404-E-009-02. We appreciate Dr. J. Keenan for the RBS analysis and Dr. W.C. Chen and F.C. Wu for assistance in the TEM.

References

[1] P. Kofstad, *J. Electrochem. Soc. 109* (1962) 579.
[2] A.G. Revesz, J.F. Allison and J.H. Reynolds, *Comsat. Tech. Rev., 6* (1976) 57.
[3] H. Terui and M. Kobayashi, *Appl. Phys. Lett., 32* (1978) 666.
[4] G.M. Choi, H.L. Tuller and J.S. Haggerty, *J. Electrochem. Soc., 136* (1989) 835.
[5] A.J. Moulson and J.M. Herbert, *Electroceramics; Materials, Properties, Applications*, Chapman and Hall, London, p. 197.
[6] K. Ohta, K. Yamada, K. Shimizu and Y. Tarui, *IEEE Trans. Electron Dev., 29* (1982) 368.
[7] H. Shinriki, T. Kisu, S. Kimura, Y. Nishioka, Y. Kawamoto and K. Mukai, *IEEE Trans. Electron Dev., 37* (1990) 1939.
[8] C.A. Steidel and D. Gerstenberg, *J. Appl. Phys., 40* (1969) 3828.
[9] G. Oehrlein, *Thin Solid Films, 156* (1988) 207.
[10] T. Kato and T. Ito, *J. Eelctrochem. Soc., 135* (1988) 2586.
[11] M. Matsui, S. Oka, K. Yamagishi, K. Kuroiwa and Y. Tarui, *Jpn. J. Appl. Phys., 27* (1988) 506.
[12] H. Shinriki and M. Nakata, *IEEE Trans. Electron Dev., 38* (1991) 455.
[13] E. Kaplan, M. Balog and D. Frohman-Bentchkowsky, *J. Electrochem. Soc., 129* (1976) 1570.
[14] S. Byeon and Y. Tzeng, *Tech. Dig., 1988 IEEE IEDM*, IEEE, New York, p. 722.
[15] K. Sunohara and H. Morita, *Jpn. J. Appl. Phys., 30* (1991) 3729.
[16] T. Kallfass and E. Lueder, *Thin Solid Films, 61* (1979) 259.
[17] S. Seki, T. Unagami and O. Koguye, *J. Electrochem. Soc., 132* (1985) 3054.
[18] S. Seki, T. Unagami, O. Kogure and B. Tsujiyama, *J. Vac. Sci. Technol. A, 5* (1987) 1771.
[19] U. Teravaninthorn, Y. Miyahara and T. Moriizumi, *Jpn. J. Appl. Phys., 26* (1987) 347.
[20] G.S. Oehrlein, F.M. d'Heurle and A. Reisman, *J. Appl. Phys., 55* (1984) 3715.
[21] T. Kato and T. Ito, *J. Electrochem. Soc., 135* (1988) 2586.
[22] B.-W. Shen, I.-C. Chen, S. Banerjee, G. Brown, J. Bohnman, P.-H. Chang and R. Doering, *Tech, Dig., 1988 IEEE IEDM*, IEEE, New York, p. 582.
[23] S. Roberts, J. Ryan and L. Nesbit, *J. Electrochem. Soc., 133* (1986) 1405.
[24] S.-I. Kimura, Y. Nishioka, A. Shintani and K. Mukai, *J. Electrochem. Soc., 130* (1983) 2414.
[25] W.D. Westwood, N. Waterhouse and P.S. Wilcox, *Tantalum Thin Films*, Academic Press, London, 1975.
[26] D.A. Vermilyea, *J. Electrochem. Soc., 104* (1957) 542.
[27] N.F. Jackson, *J. Appl. Electrochem., 3* (1973) 91.
[28] R.E. Pawel and J.J. Campbell, *J. Electrochem. Soc., 111* (1964) 1230.
[29] S. Tanimoto, M. Matsui, K. Kuroiwa and T. Tarui, *J. Electrochem. Soc., 139* (1992) 320.
[30] C.C. Wang, K. Zaininger and M.T. Duffy, *RCA Rev., 31* (1970) 728.
[31] W.H. Knausenberger and R.N. Tauber, *J. Electrochem. Soc., 120* (1973) 927.
[32] P.-H. Chang, H.-Y. Liu, J.A. Keenan, J.M. Anthony and J.G. Bohlman, *J. Appl. Phys., 62* (1987) 2485.
[33] *Powder Diffraction File 25-922*, International Center for Diffraction Data, Swarthmore, PA, 1993.
[34] F.J. Wu, *MS Thesis*, National Chiao Tung University, Hsinchu, 1992.
[35] H. Gleiter, in R.W. Cahn and P. Hassen (eds.), *Physical Metallurgy*, 3rd edn., Elsevier, Amsterdam, 1983, p. 684.